

# Piezoelectrically modulated touch pressure sensor using graphene barristor

Hyeon Jun Hwang<sup>1</sup>, So-Young Kim<sup>1,2</sup>, Soo Cheol Kang<sup>1,2</sup>, Billal Allouche<sup>1</sup>, Byoung Hun Lee<sup>1,2</sup>

<sup>1</sup> Center for Emerging Electronic Devices and Systems,

<sup>2</sup>School of Material Science and Engineering, Gwangju Institute of Science and Technology

Cheomdan-gwagiro, Buk-gu, Gwangju, 61005, South Korea

Phone: +82-62-715-2347 E-mail: bhl@gist.ac.kr

## Abstract

A Piezoelectric polymer(PVDF-TrFE) gated touch pressure sensor using graphene-Si Schottky junction barristor has been demonstrated by combining the high on-off ratio over  $10^2$  and low leakage current characteristics. Its performances were optimized by presetting the initial Fermi level of graphene using a polymer doping process. The sensing current modulation ratio was maximized to 312% under 3Mpa touch pressure.

## 1. Introduction

Graphene, 2D sheets of carbon atoms, has been investigated for a wide range of applications because of its exceptional properties such as high carrier mobility, excellent thermal conductivity and mechanical strength [1-3]. Furthermore, the linear relationship between an external bias and carrier concentration near the Dirac point can be utilized in various interesting electronic applications because the conductivity of graphene can be modulated in a predictable way even with a small change in the Fermi level [4-6]. In this work, we demonstrate a touch sensor device using a piezoelectric copolymer, PVDF-TrFE, as a gate for graphene-Si barristor to improve the sensitivity of touch sensor. The piezoelectric potential created by and externally applied force to the PVDF-TrFE layer acts as a gate modulation voltage controlling the carrier transport in a graphene-silicon interface.

## 2. Experiment

To fabricate the graphene-Si barristor, monolayer CVD graphene was transferred to a 90nm SiO<sub>2</sub>/n-type silicon substrate using a wet transfer method. Graphene channel was patterned using Au hard mask and O<sub>2</sub> plasma etching. And then, active window regions (W/L=14/16 μm) were defined using photolithography and exposed buffered oxide etchant. As SiO<sub>2</sub> underneath the graphene channel is removed, graphene and exposed silicon substrate were brought into contact and the Schottky junction with a minimal interfacial could be fabricated. Au source and drain electrode were defined by e-beam evaporator deposition, photolithography. For chemical doping, devices were immersed in different poly (acrylic acid) (PAA) aqueous solutions (0.002, 0.02, 0.2 and 2.5wt%) for three hours. After the doping, samples were rinsed using ethanol for 1~2 seconds in order to eliminate eventual chemical residues. Then, Al<sub>2</sub>O<sub>3</sub> dielectric was deposited using atomic layer deposition(ALD) and annealed at 300°C for 1 hour in order to densify the Al<sub>2</sub>O<sub>3</sub> layer and remove residual water molecules. Following, Au gate electrode was patterned by e-beam evaporation and lift off photolithography process. Piezoelectric copolymer, PVDF-TrFE (75:25), was spin-coated on Au bottom electrode followed by a thermal anneal at 140°C for 1hour to improve the crystallinity and remove the residual

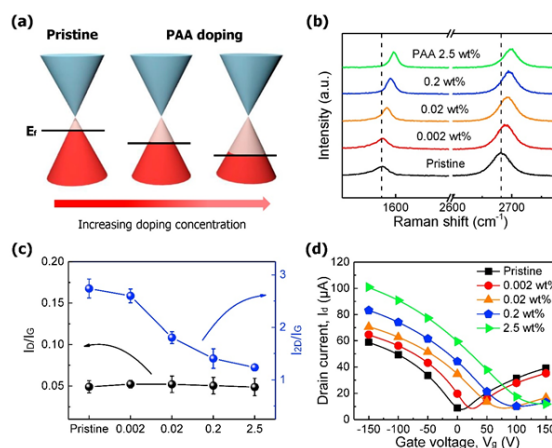


Fig. 1 (a)Schematic of Fermi level of graphene by PAA doping. (b) Raman spectra of single layer graphene samples taken before and after the PAA doping. (c)  $I_{D}/I_G$  and  $I_{2D}/I_G$  ratio of graphene at each PAA doping concentration. (d) Transfer curve of GFET at each PAA doping concentration.

solvent. Finally, top electrode for metal/piezoelectric/metal (MPM) structure was deposited using a thermal evaporator. For the initial poling of PVDF-TrFE thin film, a strong electric field around 80~100MV/m was applied for at least 20 minutes.

## 3. Results

Fig. 1a schematically illustrates how the Fermi level in graphene is modulated by PAA doping. This p-type doped graphene was deduced from the Dirac point shift in IV curves. Fig. 1b shows the Raman spectra of the pristine graphene and PAA doped graphene with various concentration of PAA. The full width at half maximum (FWHM) of the 2D peak is about 32 cm<sup>-1</sup>, and the ratio of 2D/G peak intensities is about 2.74, indicating the monolayer graphene and damage-free characters of graphene post doping process. Both G and 2D peak were shifted from 1584 to 1599 cm<sup>-1</sup>, and from 2683 to 2699 cm<sup>-1</sup> in the PAA doped graphene at concentration of 2.5wt% due to the shift in the phonon frequencies with doping. In addition, FWHM of the G peak gradually decreased from 17.82 to 8.45 cm<sup>-1</sup>. It has been reported that the blue shift of G and 2D peak positions and the narrowing of the G peak can be attributed to p-type doping in a single layer graphene [7]. After the PAA doping, the intensity of the 2D peak remains very high whilst that of the D peak is negligible (Fig. 1b). This demonstrates that the doping did not affect the graphene quality. Fig.1c shows that  $I_{2D}/I_G$  changes from 2.74(pristine) to 1.23(PAA 2.5wt% doping). This slightly decrease in the  $I_{2D}/I_G$  ratio is due to the doping effect, consistent with the trends observed by the Raman spectra for doped graphene [7].

Also, the small change of  $I_D/I_G$  ratio from 0.049 to 0.052 under the different doping concentrations indicates relatively low defect density. All these results show successful doping of the graphene without significant damages to its lattice structure. To investigate the electrical properties of the doped graphene, the electrical response of back-gate GFETs doped with different PAA concentration (0.002~2.5wt%) was measured, Fig. 1d. Before the PAA doping, the Dirac point of GFETs was located at around 13.4V, which indicates that the graphene is slightly doped with holes. As the concentration of PAA increases, the Dirac point of  $I_d$ - $V_g$  curve gradually moved leftwards from 13.4 to 150V at PAA 2.5wt% doped, resulting in a downward shift in the Fermi level of graphene, i.e. much stronger p-type doping.

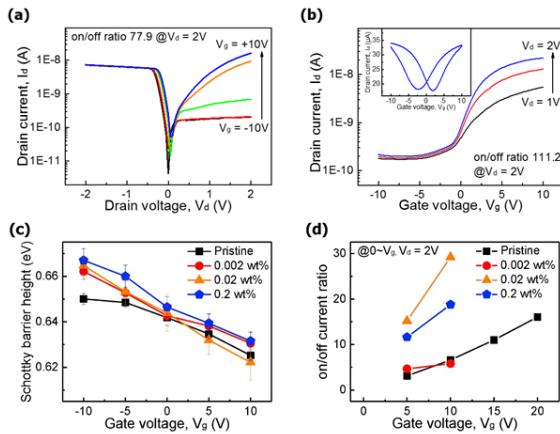


Fig. 2 (a)  $I_d$ - $V_d$  curves of graphene barristors with PAA 0.02 wt% doped graphene. (b)  $I_d$ - $V_g$  curves of graphene barristors at different drain voltages. (c) The variation of Schottky barrier height as a function of the  $V_g$ . (d) The on-off ratio of graphene barristor at each doping process.

Fig. 2a shows the output characteristics of the graphene barristor with PAA 0.02 wt% doping. Typical rectifying diode behavior was observed in a wide gate bias range. As the gate voltage was modulated, the current level changed by 77.9 times. The transfer characteristics of GFETs fabricated with the graphene barristor showed hysteretic behavior and on-off ratio was only 1.83 due to high residual charges. On the other hand, very high on-off ratio, over 110, was obtained in graphene barristor shown in Fig.2b. The variations of barrier height and the on-off current ratio as a function of  $V_g$  for the graphene barristor with different doping concentrations were summarized in Fig. 2c and Fig. 2d.

The operation principle of the piezoelectric gated graphene barristor in response to external force is shown in Fig. 3a. Initially, the graphene Fermi level is located below the Dirac point due to p-type doping occurred during the device fabrication process. When the vertical force is applied to pre-poled PVDF-TrFE layer, the polarization of PVDF-TrFE is expected to generate dipoles with modulate the Schottky barrier height. If electrons are induced in graphene, then the Fermi level shifts to upper state, resulting in the decrease in Schottky barrier height. Therefore, the change of the current flow in the  $I_d$ - $V_d$  curves under various forces is due to the modification of Schottky barrier height by piezoelectric potential of PVDF-TrFE layer. Fig. 3b shows the representative

$I_d$ - $V_d$  curves of graphene barristor having a PVDF-TrFE layer with various pressure loading from 100g to 1kg. At a 1 kg load condition, the amount of current modulation by the pressure load increased by 6.96 times, which is about 7 times higher than the value obtained from GFETs with PVDF-TrFE case. Since the actual charge coupling ratio between the dipole charge and gate electrode is not accounted, the actual potential change would be higher than the estimated value. Fig. 3c shows the drain current change of PVDF-TrFE/graphene barristor under a repetitive press test. The current was measured with 1 kg press weight for 10 s dwell time at  $V_g = 0$  V and  $V_d = 2$  V. When 1 kg load applied, the drain current change in graphene barristor was 25.4 %.

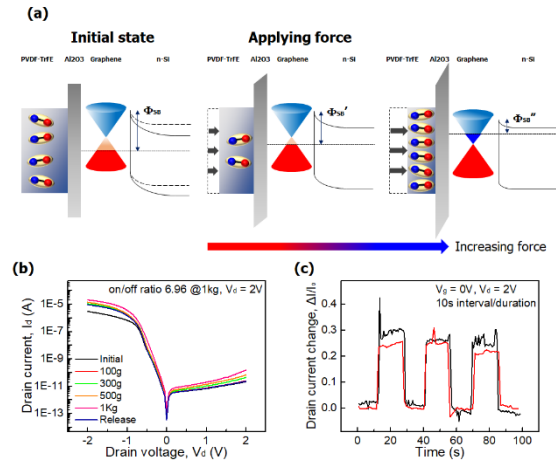


Fig. 3 (a) Schematic operation principle of piezoelectric gated graphene barristor. (b)  $I_d$ - $V_d$  curves of graphene barristor in response to various press weights, the drain current at reverse bias increased as increasing press weight. (c) Time-dependent drain current change of graphene barristor based touch sensor with repetitive press/release test,  $V_g = 0$  V,  $V_d = 2$  V, 1 kg of press weight and 10s of press duration time.

### 3. Conclusions

By implementing the control of the Schottky barrier height of graphene barristor via PAA doping, the PVDF-TrFE/graphene barristor hybrid stacked device can be more easily modulated by the external force. Since graphene can be integrated in large scale touch panels or flexible electronic skin devices, we believe that PVDF-TrFE/graphene barristor stack is a very promising hybrid candidate for sensitive force/pressure touch sensor, force/pressure monitor and touch screen technologies.

### Acknowledgements

This work was supported by Nano Materials Technology Development Program (2016M3A7B4909941) and Creative Materials Discovery Program on Creative Multilevel Research Center (2015M3D1A1068062) through the National Research Foundation(NRF) of Korea funded by the Ministry of Science and ICT.

### References

- [1] Y. Zhang et al., Appl. Phys. Lett., (2005) 86, 073104
- [2] P. Neugebauer et al., Phys. Rev. Lett., (2009) 103, 136403
- [3] D. Li et al., Nat. Nanotechnol., (2008)
- [4] H.J. Hwang et al., Nanotechnol., (2013) 24, 175202
- [5] J.H. Yang et al., Micro. Eng., (2015) 147, 79
- [6] W. Park et al., Nanotechnol., (2013) 24, 475501
- [7] R. Beams et al., J. Phys.: Condens. Matter, (2015) 27, 083002